Stress effects of silica particles in a semiconductor package molding compound

110th European Study Group with Industry,
28th June - 3rd July, 2015
University of Limerick, Ireland

Authors:

Francesc Font[1,9], Graeme Hocking[2], David A. Burton[3], Vincent Cregan[4], Pavel Iliev[5]

Workshop contributors:

Paul Dellar[6], Shishir Suresh[7], Shaunagh Downing[7], Matthew Haynes[1], Helena Ribera[4], Robert Mangan[7], William Lee[1], Stephen O'Brien[1]

Industry Representative:

Patrick Elebert[8]

[1]MACSI, Department of Mathematics & Statistics, University of Limerick, Limerick, Ireland
[2]School of Chemical and Mathematical Sciences, Murdoch University, Perth, Australia
[3]Department of Physics, Lancaster University, Lancaster, UK
[4]Centre de Recerca Matematica, Barcelona, Spain
[5]University of Sofia, Sofia, Bulgaria
[6]OCIAM, Mathematical Institute, University of Oxford, Oxford, UK
[7]University of Limerick, Limerick, Ireland
[8]Analog Devices, Ireland
[9]francesc.font@ul.ie

Summary

The stresses induced on a silicon chip encased in an epoxy compound are considered due to absorption of moisture and the presence of silica particles in the coating. A range of different approaches are considered including a one-dimensional model for the curvature due to the absorption of water in a bi-lateral sheet, numerical simulations for the stress at the molding compound-silicon die interface and a two-dimensional model in the complex plane.

Contents

1 Introduction

Analog Devices manufacture silicon chips which are used in a variety of circumstances. The chips (or die) do not come as a single entity but have electrodes on top and sit on a copper paddle, all of which is then packaged within plastic. Either the whole thing is encased or alternatively the plastic may be put over the top with the copper paddle as a base (Figure 1). The plastic is an epoxy molding compound that consists of the plastic and up to 90% filler particles that are made of silica.

During manufacture the whole package is heated to a high temperature and then cooled down to room temperature for use. In this process the package is subjected to significant forces as the difference in rates of thermal expansion between the die and the plastic causes the package to bend slightly. This is expected and is a normal part of the process. The purpose of the silica particles is to minimize the effect of the differences in thermal expansion between the two materials. The filler particles are uniformly distributed in the compound and come in a range of sizes, between 50 and 100 microns (Figure 1). To give an idea of scale in the figure, the copper paddle is approximately 200 microns high. After this phase the properties of the chip are adjusted by reconfiguring the electronics to have the required design properties. It is at this point that the chips are shipped for use.

It is apparent that in certain situations the behaviour of the electrical properties of the chip deteriorate in-situ, sometimes leading to bad performance and sometimes to failure. One possible reason for this is thought to be the absorption of moisture into the epoxy compound. It is thought that this leads to a slight further bending (or perhaps unbending) of the package causing further stresses on the chip circuitry, and it is believed that it is the silica filler particles that are the dominant factor in causing problems. Electrical components are susceptible to mechanical stress and so the presence of one or more large silica particles near to the die may lead to changes in the behaviour. It is even possible that a collection of small particles may cause problems.

Analog Devices have performed a series of tests involving the placement of a buffer coating between the epoxy compound and the die to see if this would mitigate the impact of such silica particles. It was found that this coating had to be quite thick before it had any beneficial effect. They also tested the moisture absorption of the plastic compound and found it to absorb water (although the silica particles do not absorb water).

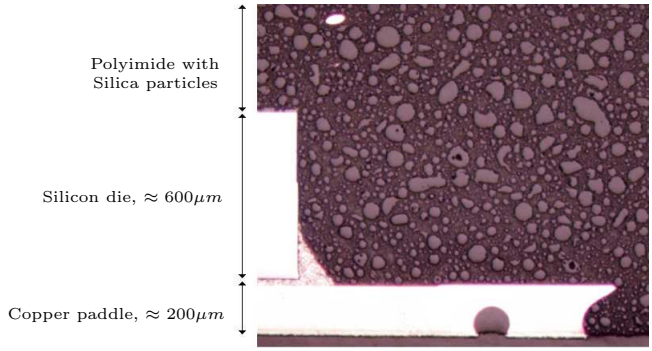

Figure 1: The setup of one end of the chip, showing the copper paddle, the die and the epoxy compound. The silica particles can be clearly seen in the compound as the lighter colour patches.

The study group was asked to investigate this problem by considering the stress field generated by the silica particles so that "a series of Monte Carlo simulations" might be performed by Analog Devices for different distributions of the particles, thus assisting in design of the layout of the chip.

The solid mechanics involved in this problem is quite difficult and so several different sub-problems were considered. This combination of approaches should provide some in-

sight into the process. The outline of this report is as follows. In Section 2 we describe a model for a two-layer materials problem to consider the effect of variable solid properties on the bending behaviour. Numerical simulations are presented in Section 3. Specifically, the finite element method in COMSOL was used to model the stress field near a bent plate subject to different particle configurations. In Section 4 the problem is approximated via a two-dimensional model and complex variable methods are applied. Finally, in Section 5 we provide some concluding remarks and suggested directions for future work.

2 Thin strip with variable moisture absorption

2.1 Model description

The task to consider the stress generated locally during bending of the chip and casing can be considered by examining the stress field generated by individual particles of silica near to the chip (see later), or it may be considered by looking at a simplified approach in which variations in concentration of the silica particles along the plastic component might affect the bending of the plate. The idea is that as water is absorbed (or heated) the differential absorption along the material will lead to variations in the bending moment, hence causing kinks or regions of higher curvature in the chip itself. Thus we need to develop a model of the curvature due to the absorption of water in a bi-material sheet.

Timoshenko [1] computed bending of two metals welded together with different coefficients of thermal expansion. Subsequently, other authors [2, 3, 4] considered this further, but the essential ideas were covered by [1] and so we use a similar analysis here. In [1] the behaviour of a thermostat with two metal strips welded together was determined. The beams were assumed to be thin and with uniform property along their length. The centre line was assumed to be such that there could be no relative movement between the two strips. While we are not dealing with a bi-metal strip in this work, we still have a very low aspect ratio and so the general assumptions of the model are valid.

One way to interpret his work is to consider it as an analysis of a very small segment of a longer strip pair where the strips have different properties. In that way the expression derived for the curvature can be treated as local. Appending pieces with different properties either side (with an assumption of continuity) leads to a modified equation for the distortion of the strip, one that now has properties that depend on lengthwise direction, x.

Timoshenko's formula for the radius of curvature ρ as shown in Figure 2 can be written as

$$\frac{1}{\rho} = \frac{2h(\alpha_1 - \alpha_2)(T - T_0)}{h^2 + 4(E_1 I_1 + E_2 I_2)\left(\frac{1}{E_1 h_1} + \frac{1}{E_2 h_2}\right)}, \tag{1}$$

where in layers $k = 1, 2$, α_k is the thermal expansion coefficient, $E_k I_k$ is the flexural rigidity and h_k is the layer thicknes. Temperature, T, is assumed uniform throughout both layers and $h = h_1 + h_2$ is the total thickness. He used this model to compute the bending due to the differential in thermal expansion between the two layers.

Modifying his analysis to consider continuous variations in material properties along the strip allows the development of an equation for the variations in behaviour of the two materials. For example, the two thermal expansion coefficients can be made a function of x, leading to differential bending along the strip. This change leads to a differential equation for the bending of the strip, given by

$$\frac{d^2 y}{dx^2} = \frac{2h(\alpha_1(x) - \alpha_2(x))(T(x) - T_0)}{h^2 + 4(E_1 I_1 + E_2 I_2)\left(\frac{1}{E_1 h_1} + \frac{1}{E_2 h_2}\right)}, \tag{2}$$

where $y(x)$ is the displacement along the strip. Note that now the thermal expansion coefficients and temperature are designated as being functions of x. The variation may

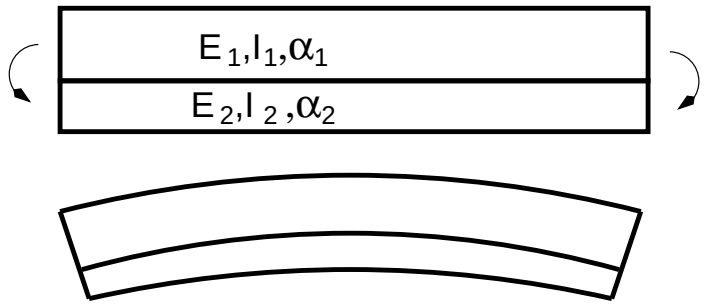

Figure 2: Sketch of the bending due to differential thermal expansion during heating or moisture absorption in two layers welded together. E is Young's modulus, I is moment and α is the thermal expansion coefficient.

also affect the rigidity, but for now we assume this effect is minor.

This equation can be integrated to compute the variation in bending as the strip heats (or cools). Indeed, it may be possible to estimate the differential between α_1 and α_2 at any point by examining the outcome of the manufacturing process. Two boundary conditions are required to enable a solution to this equation, but they can simply be set to $y(0) = y(1) = 0$ since in this problem they are not of great importance. It would seem likely in this application that the variation in the paddle would be much less than the plastic, as the paddle is made of a single material while the plastic has two constituents. The variation in $\alpha_1(x)$ is likely to be due to the location and density of the silica particles and related to the local volume fraction that they occupy, while α_2 can be expected to remain almost constant. The length scale of these variations might be expected to be of the order of the larger particles, but could also be due to a dearth or excess of particles in one particular location.

In the problem under consideration it is the moisture content that is of concern. The epoxy will absorb moisture resulting in an expansion of the material and subsequent bending. This will lead to the same kind of variation as one might expect from the cooling process, depending on the amount of expansion and the volume occupied by the silica.

Following the same derivation as for the thermal equation, we can arrive at a similar equation for the moisture induced bending, where the terms involving α_k are replaced by a moisture interaction of the form $\beta_1(x)(W_1 - W_{10}) - \beta_2(x)(W_2 - W_{20})$, where $\beta_k, k = 1, 2$ is the expansion factor as water is absorbed and $W_{k0}, k = 1, 2$ is the initial water concentration in each component. However, since we do not expect the copper to change, this term in layer 2 will disappear, giving

$$\frac{d^2y}{dx^2} = \frac{2h\beta_1(x)(W_1(x) - W_{10})}{h^2 + 4(E_1I_1 + E_2I_2)\left(\frac{1}{E_1h_1} + \frac{1}{E_2h_2}\right)}, \tag{3}$$

if we assume that the presence of the moisture has no influence on the other properties of the components. In fact, it is relatively simple to include the variation of the properties if we know the relation, but it is unlikely that it will be of sufficient magnitude to change the results. The moisture term can be replaced by

$$B(x) = \beta_1(x)(W_1(x) - W_{10})\,,$$

to test whether it is likely to make a difference, since it is simply a function of x that is related to the volume fraction of silica along the epoxy layer.

2.2 Results

Figure 3 shows three different cases in which the variability of silica concentration induced different outcomes. In each case the dashed line represents the curve resulting from a

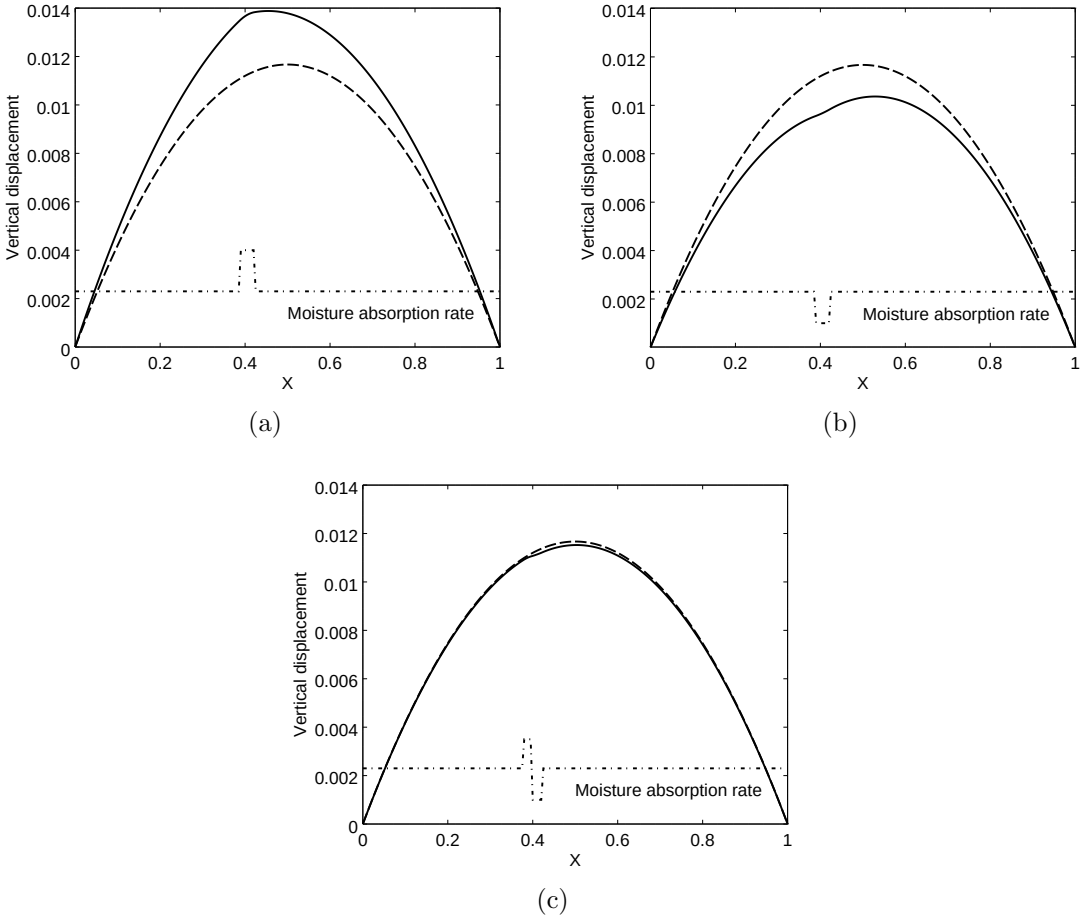

Figure 3: Comparison of three cases of variable moisture uptake along the epoxy side of the component. The dot-dash line indicates the variation in moisture. The dashed line gives the bending for the uniform case and the solid line is the result of the variable moisture uptake (due to the variation in silica concentration). Other parameters; $E_1 = 18\,\mathrm{GPa}$, $E_2 = 120\,\mathrm{GPa}$, $h_1 = 0.008\,\mathrm{m}$, $h_2 = 0.001\,\mathrm{m}$ and $I = h^3/12$.

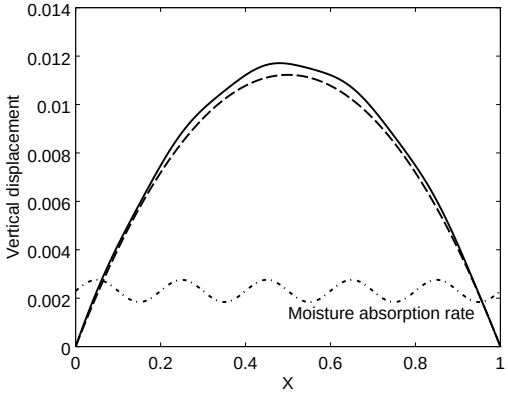

Figure 4: Distortion due to sinusoidal variation in the moisture expansion rates. The plate is now quite "wobbly".

uniform situation. In frame (a), there is one patch where there is a dearth of silica, so that the expansion coefficient is higher causing greater curvature at that point. The extra bending causes a greater arc in the whole system, but that is due to the sharpish corner that develops. In frame (b), there is a region of lower shrinkage (high silica region) close to $x = 0.4$, and a narrow region of high absorption. On this occasion the non-uniform case has slightly less bending but a slight kink in the shape is clear. Finally, in frame (c) is shown an example in which the paucity and excess regions are next to each other (as might happen if there were some repositioning of the silica in the manufacturing process). In this case the change in shape is quite localized to this region, but involves the formation of a rather severe kink in the system.

In a final example (Figure 4) we consider a rather extreme case in which there is some continuous variation in the density of silica along the bi-material. Here the variation in expansion is causing some quite nasty kinks to form. It is possible that shorter wavelength inconsistencies can cause more dramatic bending.

2.3 Conclusions

These examples show that if there is variation in the volume fraction along the length of the coating it may result in extra stresses on the chip itself due to this extra, localized bending. The variation may be caused by near proximity of several large particles thus causing an increased local concentration of silica. It is also worth noting that any effect due to this will occur in the same place in both the cooling phase during manufacture and in any subsequent moisture absorption. While the "damage" done during manufacture can be repaired, it is not possible to repair the later damage due to moisture absorption. It is even possible that given the right circumstances the two effects could be additive, even though the process of cooling and moisture absorption would result in bending in the opposite directions.

If this mechanism proves to be a reasonable possibility, it might show up in the amount of "remedial" work required after manufacture, i.e. those components requiring the most adjustment post-manufacture may be showing signs of this variability in silica volume fraction and so it is these that may be most likely to fail later. Note that all of this work assumes that the chip is kept well away from the ends of the paddle where stress effects can be expected to be large. There is an assumption that the area of interest is away from the ends. This model does not take into account bending in the lateral direction where there may also be variations in local properties. In order to determine the relevance of this factor it would be worth estimating the variability in "density" along the length to determine if it is sufficient to cause the bending required to cause the observed damage. If it turns out to be unlikely due to the uniformity of the particle distribution, then it

will be necessary to return to the more time consuming calculation of the stresses due to individual particles.

3 Numerical simulation for Stress field at epoxy molding-silicon die interface

3.1 Model description and numerical scheme

In this section we use the finite element method (FEM) in COMSOL to analyse and simulate the stress near the interface of the epoxy molding and the silicon die as a result of the silica particles embedded in the molding. We consider a two-dimensional, stationary model to predict the stress field. Two different particle configurations are studied. Firstly, in case A (Figure 5(a)) we investigate the relationship between one particle and the stress in the molding. Next, in case B we examine the impact of two particles on the stress field (Figure 5(b)).

The starting point is the construction of the problem geometry. The domain consists of two subdomains, namely a rectangle for the molding and a circle for the silica particle. As illustrated in Figure 5 the yellow area represents the molding compound, the light grey circle a silica particle and the dark grey area the silicon die. The simulation domain is the rectangle delimited by the dashed line. The height and length of the rectangle are $h_1 = 1000\,\mu$m and $h_2 = 5000\,\mu$m, respectively. The Cartesian coordinate system is used to describe the problem with the geometry aligned such that the length is described along $x \in [-h_2/2, h_2/2]$ and the height $y \in [0, h_1]$. The radius of the particle is $r = 25\,\mu$m. In both configurations, d represents the vertical distance from the base of the rectangle to the lowest point on the surface of a particle. With respect to case B, l denotes the horizontal distance between two particles. The COMSOL materials library is used to define the material properties of both the molding and silica particles. For the molding we use the material *Epoxy-50% silica particles* to approximate the molding used by Analog Devices. A summary of the physical dimensions and material parameters is given in Table 1.

Quantity	Symbol	Value	Units
Molding height, length	h_1,h_2	1×10^{-3}, 5×10^{-3}	m
Particle radius	r	2.5×10^{-5}	m
Young's modulus of epoxy, silica	E_e, E_s	72.9×10^9, 18.03×10^9	Pa
Poisson ratio of epoxy, silica	ν_e, ν_s	0.17, 0.23	-
Density of epoxy, silica	ρ_e, ρ_s	2203, 1100	$\mathrm{kg\,m^{-3}}$

Table 1: Dimensions of geometry and material properties of molding compound (Epoxy-50% silica particles) and silica used in simulations.

To reduce model complexity we use the following assumptions. Firstly, we simplify the geometry of the problem by neglecting the die and copper paddle located at the base of the molding. We assume that both the molding and silica particles are linear elastic materials such that strains vary linearly with stresses.

We use the solid mechanics module in the structural mechanics package to simulate the stress field. The governing equations are

$$-\nabla \cdot \sigma = F_V\,, \qquad \sigma = \boldsymbol{s}\,, \qquad \boldsymbol{s} = \mathbf{C} : (\epsilon - \epsilon_{inel})\,, \qquad \epsilon = \frac{1}{2}[(\nabla \boldsymbol{u})^T + \nabla \boldsymbol{u}]\,, \qquad (4)$$

where σ is the Cauchy stress tensor, F_V is the body force per unit volume, ϵ is the infinitesimal strain tensor, $\mathbf{u}$ is the displacement (or strain) vector and $\mathbf{C}$ is the fourth-order elasticity (or stiffness) tensor. The first equation in (4) is the equation of motion,

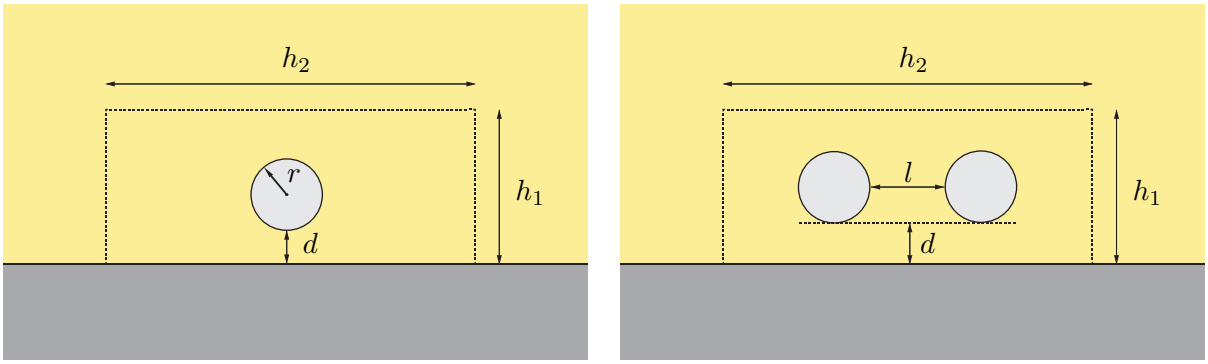

(a) (b)

Figure 5: Sketch of case A and case (b). The yellow area represents a portion of the molding compound (Epoxy-50% silica particles), the light grey circle a silica particle and the dark grey area the silicon die. The simulation domain is represented by the rectangle delimited by the dashed line.

which is an expression of Newton's second law. The third equation is Hooke's law, which relates the unknown stresses and strains.

Boundary conditions are required at the four outer edges of the molding and the particle-molding interface. At $x = -h_2/2$, $x = h_2/2$ and $y = h_1$ we impose free boundary conditions so that there are no constraints or loads acting on the boundary. At the particle-molding interface we apply stress continuity. Finally, in order to model the bending caused by the the moisture absorption in the epoxy, we impose a prescribed displacement condition of the form $u = -\varepsilon x^2$ at the lower surface of the molding, $y = 0$. The small, dimensionless parameter $\varepsilon = 1 \times 10^{-10}$ determines the magnitude of the overall displacement of the molding.

The next step is the discretisation of the original problem which consists of transforming the continuum problem as represented by the partial differential equation model into a discrete problem in finitely many variables. The domain is subdivided into finite elements of variable size and shape which are interconnected by a finite number of nodal points. COMSOL automatically partitions the domain into small finite elements of simple shape. The resulting partition is referred to as the finite element mesh (Figure 6). In two dimensions the mesh subdivides the domain into triangles. However, this is only an approximation as part of the domain close to the particle is curved. The sides and corners of the triangles are called mesh edges and mesh vertices, respectively. In each finite element the unknown stress is approximated by some low order interpolating polynomial in such a way that the stress is defined in terms of the approximate stresses at the vertices. For the current problem COMSOL used a mesh of 7156 elements. This mesh size was selected as successive, finer meshes showed no significant change predicted stress.

We performed simulations for the one and two particle configurations. We chose the parameter sweep option to simulate the stress field for varying molding parameters. Specifically, for case A the simulation was carried out several times for different values of d. For case B, d was fixed and simulations for varying l were performed.

3.2 Discussion

The results from the simulations are shown in Figures 7-11. Figure 7 shows the stationary stress field in the molding for one silica particle. The largest stresses are located near the edges of the molding at $x = -h_2/2$ and $x = h_2/2$. These high stresses are due to the displacement boundary condition, $u = -\epsilon x^2$, at the lower surface of the molding, and thus are not caused directly by the particle. Hence, for the remainder of the discussion

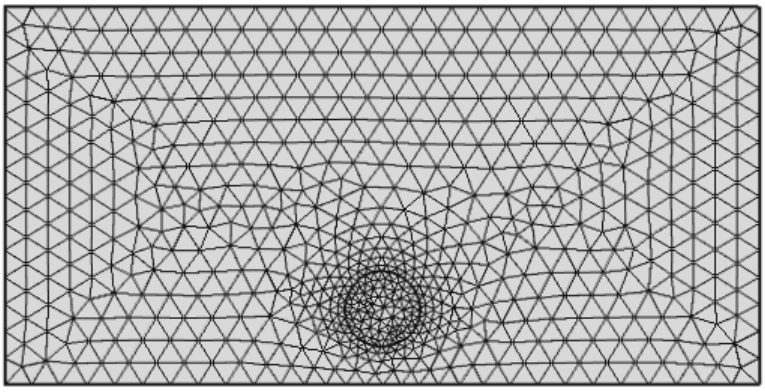

Figure 6: FEM mesh for domain with one particle. The mesh consists of 7156 mesh elements and was constructed systematically using COMSOL's mesh mode.

we neglect the stress field near the edges of the molding.

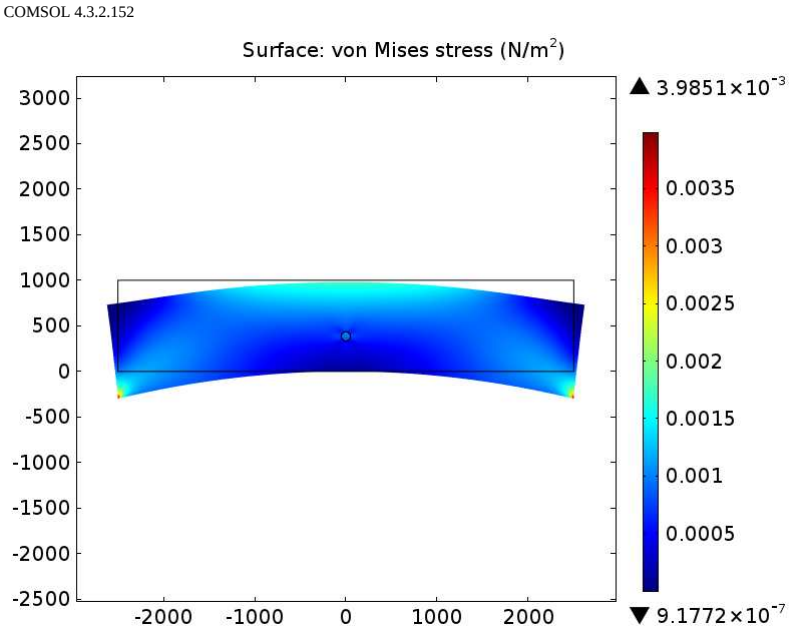

Figure 7: Stress field in molding subject to one particle.

Figure 8 shows the stresses for case A near the centre of the molding along $y = 0$. The different coloured curves denote solutions for varying d. In particular, we performed simulations for $d = 5\,\mu$m (blue), $10\,\mu$m (green), $15\,\mu$m (red), $20\,\mu$m (cyan) and $25\,\mu$m (magenta). Figure 8 reveals that the stress decays rapidly for increasing values of d. This fact is corroborated by Figure 9 which shows the stress at the origin for varying d. Smaller values of d lead to higher stresses.

The stress field for case B near the centre of the molding along $y = 0$ is shown in Figure 10. The coloured curves represent solutions for fixed $d = 5$ m and varying l. We carried out simulations for $l = 5\,\mu$m (blue), $30\,\mu$m (green), $55\,\mu$m (red), $80\,\mu$m (cyan), $105\,\mu$m (magenta), $205\,\mu$m (yellow) and $505\,\mu$m (black). The graph suggests that in each case the highest stresses at the die-molding interface are located directly beneath the particles. Figure 11 illustrates the stresses for case B along $y = 0$. The horizontal distance between the two particles is fixed at $l = 10$ m, and d is varied such that $d = 5\,\mu$m (blue), $10\,\mu$m (green), $15\,\mu$m (red), $20\,\mu$m (cyan) and $25\,\mu$m (magenta). Again we note that as d decreases the stresses at the molding-die interface increase. In addition, as before, the highest stresses are located directly beneath the particles.

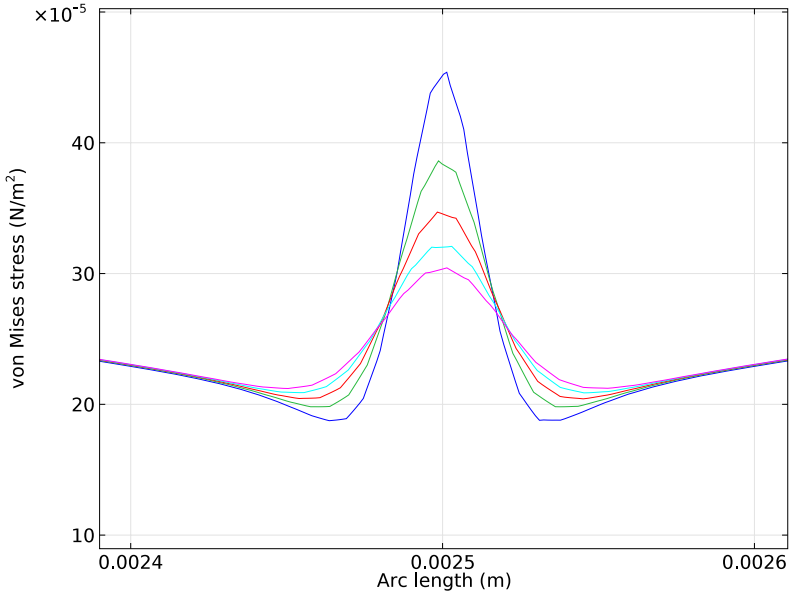

Figure 8: Stress field at the interface between the molding compound and the silicon die at $y = 0$ for $d = 5\,\mu$m (blue), $10\,\mu$m (green), $15\,\mu$m (red), $20\,\mu$m (cyan) and $25\,\mu$m (magenta).

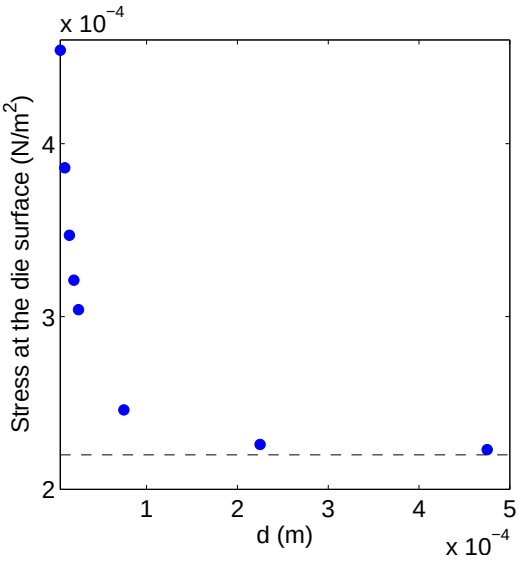

Figure 9: Stress at the central point of the interface as a function of d. The first five points on the left represent the plots from Figure 8. The remaining three points correspond to larger values of d. The black line is the stress experienced when the particle is removed.

3.3 Conclusions

In this section we presented numerical simulations for a simple two-dimensional geometry that approximates the qualitative behaviour of the semiconductor and molding compound used by Analog Devices. Neglecting the stresses near the edges $x = -h_1/2$ and $h_1/2$, we showed that in all of the considered scenarios, the highest stresses at the die-molding interface are located directly below the silica particles As the particles were moved away from the interface the stresses were shown to decay very fast. A more in depth study of this phenomena would provide valuable information on how to optimize the size of the

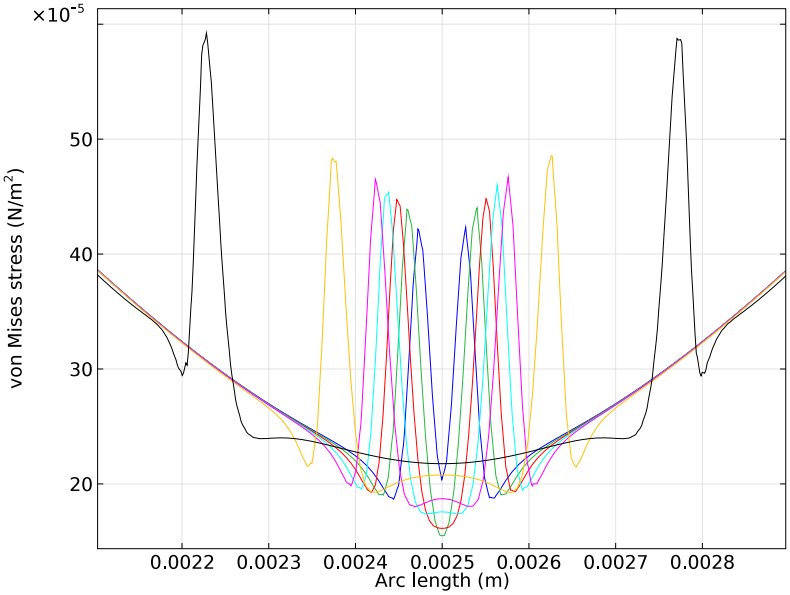

Figure 10: Stress created at the interface by the presence of the two silica particles. For this simulations the particle-interface distance is fixed at $d = 5\,\mu$m and the separation between particles is $l = 5\,\mu$m (blue), $30\,\mu$m (green), $55\,\mu$m (red), $80\,\mu$m (cyan), $105\,\mu$m (magenta), $205\,\mu$m (yellow) and $505\,\mu$m (black).

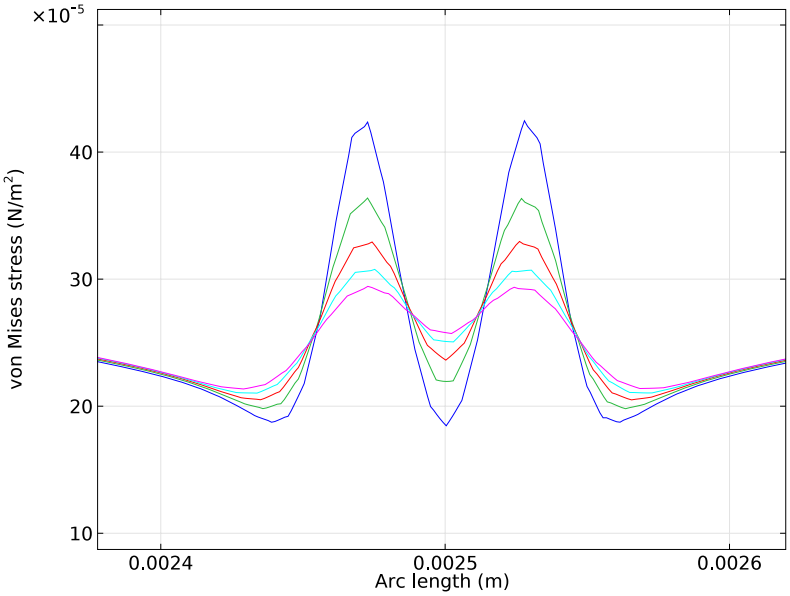

Figure 11: Stress created at the interface by the presence of the two silica particles. In this case the separation between particles is fixed at $l = 10\,\mu$m and the particle-interface distance is $d = 5\,\mu$m (blue), $10\,\mu$m (green), $15\,\mu$m (red), $20\,\mu$m (cyan) and $25\,\mu$m (magenta).

intermediate layer separating the silicon chip and the molding compound.

4 2D approximation in the complex plane

It is well-known that complex variable theory provides an elegant and powerful tool for computing incompressible and irrotational fluid flows in 2 dimensions [5]. Perhaps the

most striking application of this approach is the study of vortex dynamics; analytic continuation and conformal mapping techniques have played significant roles in highly efficient calculations of the dynamical evolution of vorticity [6], and the fluid forces exerted by vortices, in a vast array of domains with non-trivial geometries and topologies (see, e.g., [7, 8]). It is perhaps less well-known that such techniques can be fruitfully brought to bear on problems in elasticity theory, as first demonstrated by Kolosov and Muskhelishvili in 1909 (see [9] and references therein). The strategy that we follow here is inspired by their treatment of elasticity in the complex plane, as presented in Ref. [9], but with modifications that accommodate thermal stress.

The purpose of these notes is to explore the thermo-mechanical response of a simple idealised system that captures a flavour of the full problem and is amenable to analytical investigation. We represent the silica particle as a disc in the complex plane and embed the disc in a finite medium representing the resin. The Lamé parameters λ, μ, the coefficient of thermal expansion α and the temperature T of the resin are constant. A thin elastic loop, with Young's modulus E, bounds the resin-particle composite and, for simplicity, we neglect the shear forces within the loop. For convenience, we suppose that the composite loop-resin-particle system has finite thickness h (out of the plane) and endow the loop with a rectangular cross-section. The area of the cross-section of the loop is $A = hw$, where the width w of the cross-section is much less than the other length scales in the system, and we will capture the presence of the chip by allowing the product EA to depend on position within the loop. Of course, we do not permit any element of the loop-resin-particle system to deform out of the plane and, furthermore, the loop and the silica particle are both assumed to be inert to changes in temperature. We suppose that the silica particle is rigid when compared to the resin, and set the displacement of the resin to zero at its interface with the silica particle. We also appropriately balance the contact forces at the interface of the loop and the resin.

The small deformation of the composite system due to a change in temperature can be found by solving

$$-i\big[(\kappa+1)\Omega(Z) - 2\mu\mathcal{D} + \beta Z\big] = \frac{\mathcal{T}}{h}\frac{dZ}{ds}\,, \tag{5}$$

for the function $\Omega(z)$, which is chosen to be analytic within the region bounded by the loop. The simple closed curve $z = Z(s)$ specifies the state of the undeformed loop, where s is the arc parameter of the undeformed loop. The function $\mathcal{D}(s)$ is the displacement of the outer component of the boundary of the resin and has the form

$$2\mu\mathcal{D} = \kappa\,\Omega(Z) - Z\,\overline{\Omega'(Z)} - \kappa\,\Omega\bigg(\frac{a^2}{\overline{Z}-\overline{c}} + c\bigg) + \bigg(\frac{a^2}{\overline{Z}-\overline{c}} + c\bigg)\overline{\Omega'(Z)}\,, \tag{6}$$

and the tension $\mathcal{T}$ in the loop satisfies

$$\mathcal{T}(s) = EA(s)\,\mathrm{Re}\bigg(\frac{d\overline{Z}}{ds}\,\frac{d\mathcal{D}}{ds}\bigg)\,, \tag{7}$$

where the elastic properties of the loop at the material point s are specified by $EA(s)$. The centre of the silica particle is located at $z = c$ and a is the radius of the particle. The material constant κ of the resin is

$$\kappa = 3 - 4\nu\,, \tag{8}$$

where the Poisson ratio ν of the resin satisfies

$$\frac{\lambda}{\mu} = \frac{2\nu}{1-2\nu}. \tag{9}$$

The response of the resin to changes in temperature is determined by β where

$$\beta = -(\lambda+\mu)\alpha(T - T_0)\,, \tag{10}$$

with T the temperature of the resin and T_0 the reference temperature.

We will now turn to the analysis of (5), (6) and (7) for a simple choice of $Z(s)$ and $EA(s)$; the derivation of (5), (6) and (7) is provided in the Appendix.

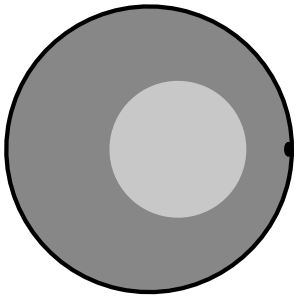

Figure 12: The silica particle (light grey) is represented by a rigid disc, and the resin (dark grey) is represented by a homogeneous isotropic thermo-elastic medium. An elastic loop (black curve) interfaces with the outer component of the boundary of the resin and captures a flavour of the presence of the chip (the black dot on the right marks the centre of the chip). The silica particle and loop are assumed to be inert to changes in temperature.

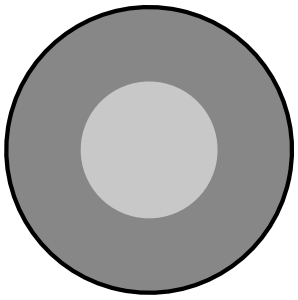

Figure 13: The axially symmetric configuration.

4.1 Application of the model

As we will now show, a perturbative analysis of (5), (6) and (7) for the configuration shown in Figure 12 yields a relatively simple analytical expression for the inhomogeneity in the tension due to the presence of the chip and the stresses due to the silica particle. It is vital to note that our model only allows the chip to sense the particle via interaction with the resin; it does not account for stresses that arise if the silica particle makes direct contact with the chip.

4.1.1 Axially symmetric solution

The simplest non-trivial solution to (5), (6) and (7) arises when the silica particle occupies the inner region of an annulus of resin (Figure 13) and the product EA is constant; thus, $c = 0$ and the loop is a circle whose centre is at the origin (for all values of the temperature T). The undeformed loop has radius b and, since s is the arc parameter of the undeformed loop, it follows

$$Z(s) = b \exp(is/b). \tag{11}$$

The function $\Omega(z)$ is chosen to be analytic inside the closed contour Z as part of the derivation of (6) and, using $\overline{Z(s)} = b^2/Z(s)$, inspection of (6) shows that $\mathcal{D}$ can be expressed as a Laurent series in Z. In particular, a purely radial deformation is described by[1] $\mathcal{D} = \delta_1 Z$ where $\mathrm{Im}(\delta_1) = 0$, and $\Omega(Z) = \alpha_1 Z$ follows from (6). Since $\mathrm{Im}(\mathcal{T}) = 0$ it

[1]Throughout this section we will label the terms of series in Z by the corresponding power of Z.

follows that (5), (6), (11) yield $\mathrm{Im}(\alpha_1) = 0$ and

$$(\chi - 1)2\mu\delta_1 + (\kappa + 1)\alpha_1 = -\beta, \tag{12}$$

$$2\mu\delta_1 = (\kappa - 1)(1 - \varepsilon^2)\alpha_1\,, \tag{13}$$

where

$$\varepsilon = \frac{a}{b}, \tag{14}$$

$$\chi = \frac{EA}{2\mu hb}. \tag{15}$$

Equation (7) leads to $\mathcal{T} = EA\,\delta_1$ and solving (12), (13) for δ_1, α_1 gives

$$\mathcal{T} = -\frac{EA}{2\mu}\frac{(\kappa - 1)(1 - \varepsilon^2)\beta}{(\kappa - 1)[\chi(1 - \varepsilon^2) + \varepsilon^2] + 2}. \tag{16}$$

Finally, using (8), (9) and (10) to eliminate κ, β yields the expression

$$\mathcal{T} = \frac{EA}{2}\frac{1 - \varepsilon^2}{(1 - 2\nu)[\chi(1 - \varepsilon^2) + \varepsilon^2] + 1}\,\alpha(T - T_0)\,, \tag{17}$$

for the tension in the loop.

It is worth noting that an approximation to (17) can be obtained using simple physical reasoning. According to Hooke's law, the tension in the loop is $\mathcal{T} = EA\,\Delta l/l$ where Δl is the increase in circumference of the loop due to the thermal expansion of the resin and l is the circumference of the loop in the undeformed state. Let r be the radius of the loop in the deformed state; thus $2\pi r = l + \Delta l$. The change in volume $\Delta\mathcal{V}$ of the resin is related to temperature as follows: $\Delta\mathcal{V} = \pi(b^2 - a^2)h\alpha(T - T_0)$. However, $\Delta\mathcal{V} = \pi(r^2 - a^2)h - \pi(b^2 - a^2)h$ and combining the previous two expressions for $\Delta\mathcal{V}$ with $r = b + \Delta r$ leads to $\Delta r = b(1 - \varepsilon^2)\alpha(T - T_0)/2$ to first order in Δr. Since $\mathcal{T} = EA\,\Delta l/l = EA\,\Delta r/b$ the result $\mathcal{T} = EA(1 - \varepsilon^2)\alpha(T - T_0)/2$ follows immediately. The additional terms in the denominator of (17) are a consequence of the back-reaction of the stretched loop on the resin; the above simple argument does not include the stress exerted by the loop on the resin in the deformed state.

An immediate consequence of (17) is $d\mathcal{T}/d\varepsilon^2 < 0$, because Poisson's ratio ν must satisfy $\nu < 1/2$, which is reassuring because the loop and the silica particle are inert under changes in temperature and less resin should lead to a lower tension.

4.1.2 Asymmetric configuration

It is straightforward to obtain the tension in the loop when the centre of the silica particle is a small distance from the centre of the circular loop in the undeformed state (Figure 12). We suppose that $\Omega(z) = \xi\alpha_0 + \alpha_1 z + \xi\alpha_2 z^2 + \mathcal{O}(\xi^2)$ where the real dimensionless parameter ξ has been introduced to easily distinguish the perturbations, and we also replace c with ξc in (6). We will set ξ to unity at the end of the calculation.

Without loss of generality we can set $\mathrm{Im}(c) = 0$ and choose $c > 0$. It follows that

$$\frac{a^2}{\overline{Z} - \xi\overline{c}} + \xi c = \varepsilon^2 Z + \xi c\left(1 + \varepsilon^2\frac{Z^2}{b^2}\right) + \mathcal{O}(\xi^2)\,, \tag{18}$$

where $\varepsilon = a/b$ as before. Hence

$$\Omega\left(\frac{a^2}{\overline{Z} - \xi\overline{c}} + \xi c\right) = \xi\alpha_0 + \alpha_1\left[\varepsilon^2 Z + \xi c\left(1 + \varepsilon^2\frac{Z^2}{b^2}\right)\right] + \xi\alpha_2\varepsilon^4 Z^2 + \mathcal{O}(\xi^2)\,, \tag{19}$$

and, using $\overline{Z} = b^2/Z$, inspection of (6) then shows that

$$\mathcal{D} = \xi\delta_0 + \delta_1 Z + \xi\delta_2 Z^2 + \mathcal{O}(\xi^2)\,, \tag{20}$$

where δ_0, δ_1, δ_2 are constants. The constant δ_0 is a uniform displacement and does not contribute to the tension of the loop, so we will not consider it further. We addressed the constants δ_1, α_1 in Section 4.1.1 and the only important new information concerns the constants δ_2, α_2. Thus, the remainder of this section is focussed on determining δ_2, α_2.

For simplicity, we will begin by assuming that EA is constant; we will introduce a modulation in EA that captures the presence of the chip at the end of this section. Note that the tension can be written as

$$\begin{aligned}\mathcal{T} &= EA\,\mathrm{Re}(\delta_1 + \xi 2\delta_2 Z) + \mathcal{O}(\xi^2) \\ &= EA(\delta_1 + \xi\delta_2 Z + \xi\overline{\delta_2}\, b^2/Z) + \mathcal{O}(\xi^2)\,,\end{aligned} \tag{21}$$

using (7), (20), $|dZ/ds| = 1$, $\overline{Z} = b^2/Z$, $\mathrm{Im}(\delta_1) = 0$. Hence, equating coefficients of ξZ^2 in (5), (6) leads to

$$EA\,\delta_2 = -hb[(\kappa+1)\alpha_2 - 2\mu\delta_2]\,, \tag{22}$$

$$2\mu\delta_2 = \kappa(1-\varepsilon^4)\alpha_2 - c(\kappa-1)\frac{\varepsilon^2}{b^2}\alpha_1. \tag{23}$$

Solving (22), (23) for δ_2, α_2 and using the results to eliminate δ_2 in $\mathcal{T}$ gives

$$\mathcal{T} = \mathcal{T}_0\left\{1 - \frac{c}{b}\frac{8\varepsilon^2(1-\nu)}{(1-\varepsilon^2)\{(3-4\nu)[\chi(1-\varepsilon^4)+\varepsilon^4]+1\}}\cos\theta\right\}, \tag{24}$$

where $\mathcal{O}(\xi^2)$ terms have been discarded prior to setting ξ to unity and $\theta = s/b$ is the angle from the real axis in the anti-clockwise sense. The constant $\mathcal{T}_0 = EA\,\delta_1$ is the tension in the loop when $c = 0$ (i.e. that given in (17)), the constant χ is given in (15), Poisson's ratio ν has been introduced using (8), and (11) has been used to show the point-wise dependence of (24). Since the parameters in (24) satisfy $\nu < 1/2$, $\chi > 0$, $0 < \varepsilon < 1$, $c/b > 0$ it follows that the tension at $\theta = 0$ is less than the tension at $\theta = \pi$. This is intuitively reasonable because there is more resin to the left of the particle than to the right of the particle (Figure 12).

It is straightforward to capture a flavour of the presence of the chip by modulating the elastic parameter EA of the loop as follows:

$$EA(s) = EA_0(1 + \gamma\cos\theta)\,, \tag{25}$$

where EA_0 is a constant and $\theta = s/b$. The centre of the chip is located at $s = 0$ and the constant γ in (25) satisfies $\gamma > 0$ to ensure that $\theta = 0$ is a maximum of EA. Equation (25) can be written as

$$EA(s) = EA_0[1 + \gamma_1 Z(s) + \gamma_1 b^2/Z(s)]\,, \tag{26}$$

where $2b\gamma_1 = \gamma$, and a repetition of the previous analysis with γ replaced by $\xi\gamma$ leads to the modification

$$EA_0\,(\delta_2 + \gamma_1\delta_1) = -hb[(\kappa+1)\alpha_2 - 2\mu\delta_2]\,, \tag{27}$$

of (22). Solving (23), (27) for δ_2, α_2 then leads to

$$\mathcal{T} = \mathcal{T}_{00}\left\{1 - \frac{8\varepsilon^2(1-\nu)c/b - \gamma\,[1+(3-4\nu)\varepsilon^4](1-\varepsilon^2)}{(1-\varepsilon^2)\{(3-4\nu)[\chi_0(1-\varepsilon^4)+\varepsilon^4]+1\}}\cos\theta\right\}, \tag{28}$$

where

$$\chi_0 = \frac{EA_0}{2\mu hb}, \qquad \mathcal{T}_{00} = \frac{EA_0}{2}\,\frac{1-\varepsilon^2}{(1-2\nu)[\chi_0(1-\varepsilon^2)+\varepsilon^2]+1}\,\alpha(T-T_0)\,, \tag{29}$$

and, as before, $\mathcal{O}(\xi^2)$ terms have been discarded prior to setting ξ to unity. Note that, to first order in the perturbation, the tension $\mathcal{T}$ is directly proportional to the temperature difference $T - T_0$.

Since $\nu < 1/2$, $\chi_0 > 0$, $0 < \varepsilon < 1$, inspection of (28) shows that the denominator of the coefficient of $\cos\theta$ is positive. However, unlike (24), the numerator has an indefinite sign because the influence of the chip and the proximity of the silica particle contribute to (28) with opposite signs (recall $\gamma > 0$, $c > 0$). It follows that a choice of parameters exists for which the inhomogeneity in the tension vanishes; the optimum position c_* of the silica particle for which this occurs is

$$c_* = \frac{b\gamma\,[1 + (3 - 4\nu)\varepsilon^4](1 - \varepsilon^2)}{8\varepsilon^2(1 - \nu)}. \tag{30}$$

4.2 Conclusions

We have developed an efficient model of a thermo-mechanical composite system that captures a flavour of the full problem. Our results are compatible with the notion that less resin is associated with lower stress and the position of the silica particle can be chosen to render the stress in the chip uniform. Although our results are intuitively reasonable, we caution that they are based on a perturbative analysis and Hertzian contact stresses between the particle and the chip are not included. We also caution that our model of the chip is somewhat crude and also does not accommodate shear forces. It can be shown that the above results are insufficient for deducing the curvature of the deformed loop (which could be used to estimate the magnitude of the shear forces in the chip) because the perturbative analysis needs to be carried through to at least second order in ξ for this purpose.

5 Summary and future work

The aim of this report was to use mathematical techniques to assist Analog Devices in developing an understanding of the stresses in a silicon chip encased in an epoxy compound due to moisture absorption and the presence of silica particles in the compound. Several different modelling approaches were considered and these will form the basis of future inquiries.

In Section 2 the stress field in the system was approximated by considering a model for the curvature due to the absorption of water in a bi-lateral sheet. The model of Timoshenko [1] was adapted to the current problem to obtain a differential equation for the vertical displacement of the strip due to thermal expansion (or equivalently absorption of water). This bulk approach was easy to implement and did not require time consuming simulations. It showed that variation in silica concentration along the length of the coating can result in extra stresses on the chip due to bending. Further work could test to what extent this variation exists in the epoxy coating and how much would be required to cause the observed damage.

In Section 3 the FEM was used to study the stress field near the epoxy molding-die interface for a reduced two-dimensional case. We have identified three possible extensions to the analysis which can be considered in future studies:

1. The largest stresses were found to be directly beneath the particles near the interface. These stresses were shown to decay very rapidly as the particles were moved away from the interface. Further analytical modelling is required to elucidate the nature of this rapid decay. Indeed, understanding this phenomena in detail would provide invaluable insight on the optimal size of the intermediate layer separating the silicon chip from the molding compound.

2. Another extension would be to include more particles in the simulations to reflect the actual particle distribution in the molding. The particles should be randomly distributed with varying sizes. Matlab can be used to generate the FEM geometry, which can then be imported into COMSOL. Preliminary results of geometries with

randomly distributed particles are shown in Figure 14. For example, Figures 14(a) and 14(b) correspond to geometries containing 1000 and 100 particles, respectively. Figures 14(c) and 14(d) show geometries where the maximum particle size was increased. Running COMSOL simulations using this geometries would provide a more realistic description of the actual process.

3. The bending of the epoxy compound was modelled by imposing a quadratic displacement at the lower boundary of the domain. This simplification was necessary to make the model tractable in the short term. In a future study, introduction of bending via a physics-based approach will make the model more representative of the actual system. In fact, COMSOL has a solid mechanics module that allows one to include thermal expansion. This would allow one to introduce bending into the model in a more realistic way.

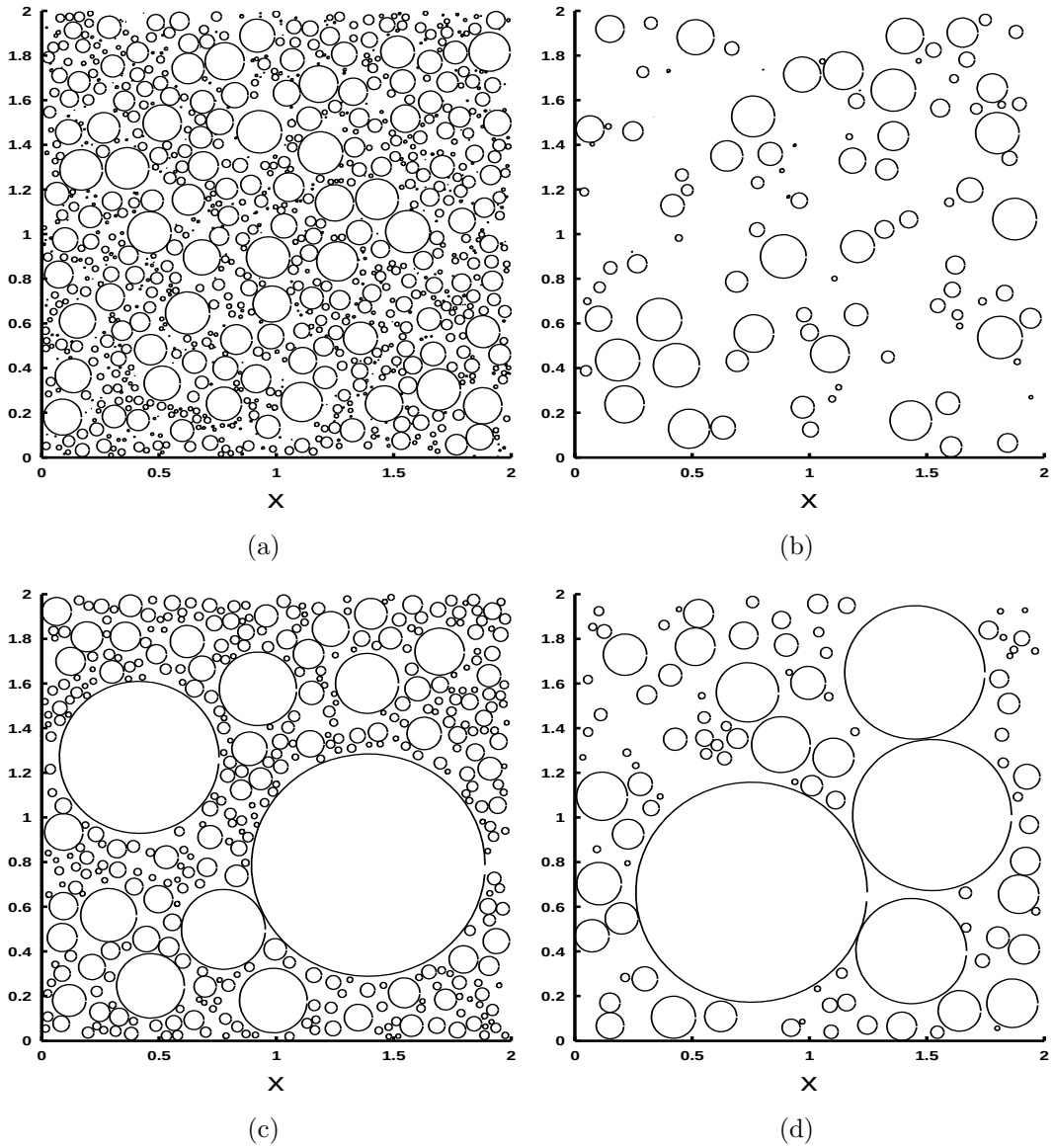

Figure 14: Particle geometry for (a) 1000 particles (b) 100 particles with minimum radius of 0.0001 and maximum radius of 0.1 and for (c) 400 particles and (d) 100 particles with minimum radius of 0.01 and maximum radius of 0.5. (Graphs were generated using dimensionless quantities.)

In Section 4 complex variable theory was used to solve a model for a thermo-mechanical composite system. The solutions indicated that less resin is associated with lower stresses.

Moreover, the position of the silica particles can be selected such that the stress in the chip becomes uniform. In a future study the model should be extended to include shear forces and Hertzian contact stresses between the particle and the chip.

The problem presented by Analog Devices proved to be demanding due to the inhomogeneity of the materials involved, and the group worked hard to come up with several different possible approaches that may lead to further progress. It is quite likely that pursuing one or more of these will lead to an answer to the questions posed.

A Derivation of complex theory elasticity model

The stress tensor σ_{jk} of the resin is

$$\sigma_{jk} = \mu(\partial_j u_k + \partial_k u_j) + \big(\lambda \partial_l u^l + \beta\big)\delta_{jk}\,, \tag{31}$$

where $j,k = 1,2$, and the vector $\boldsymbol{u}(x,y) = u_1(x,y)\hat{\boldsymbol{x}} + u_2(x,y)\hat{\boldsymbol{y}}$ is the displacement of the infinitesimal element of resin located at (x,y) in the undeformed configuration. Furthermore, $u^j = \delta^{jk}u_k$ where δ^{jk} is the Kronecker delta and the Einstein summation convention has been used.

Following the strategy in Ref. [10], the form of the constant β in (31) is fixed by demanding that σ_{jk} vanishes for a finite element of resin that is allowed to expand freely due to an increase in temperature. The expression for β is sensitive to the dimension of the ambient space; our model is constrained to 2 dimensions whereas the analysis in Chapter 1 of Ref. [10] admits thermal expansion in 3 dimensions. Thus, the expression in Ref. [10] corresponding to β will not agree with our analysis here; we will determine the form of β at the end of the Appendix.

Navier's equation

$$\mu[\nabla^2\boldsymbol{u} + \boldsymbol{\nabla}(\boldsymbol{\nabla}\cdot\boldsymbol{u})] + \lambda\boldsymbol{\nabla}(\boldsymbol{\nabla}\cdot\boldsymbol{u}) = 0\,, \tag{32}$$

follows from the local equation of momentum balance $\partial_j \sigma^j{}_k = 0$ and (31). Introducing $z = x + iy$ and the complex displacement $D(z,\overline{z}) = u_1(x,y) + iu_2(x,y)$ leads to the following:

$$\hat{\boldsymbol{x}}\cdot\boldsymbol{\nabla}(\boldsymbol{\nabla}\cdot\boldsymbol{u}) + i\hat{\boldsymbol{y}}\cdot\boldsymbol{\nabla}(\boldsymbol{\nabla}\cdot\boldsymbol{u}) = 2\partial_{\bar{z}}(\partial_z D + \overline{\partial_z D}), \tag{33}$$

$$\hat{\boldsymbol{x}}\cdot\nabla^2\boldsymbol{u} + i\hat{\boldsymbol{y}}\cdot\nabla^2\boldsymbol{u} = 4\partial_{\bar{z}}\partial_z D\,, \tag{34}$$

and (32) can be written as

$$4\mu\partial_{\bar{z}}\partial_z D + 2(\lambda+\mu)\partial_{\bar{z}}(\partial_z D + \overline{\partial_z D}) = 0. \tag{35}$$

Inspection of (35) immediately leads to

$$4\mu\partial_z D + 2(\lambda+\mu)(\partial_z D + \overline{\partial_z D}) = \phi'(z)\,, \tag{36}$$

where the unknown function $\phi(z)$ has been introduced via its derivative for later convenience.

Equation (36) and its complex conjugate can be solved for $\overline{\partial_z D}$ and the result used to eliminate $\overline{\partial_z D}$ from (36). Introducing $\Omega(z) = (\lambda+\mu)\phi(z)/[4(\lambda+2\mu)]$ in the resulting expression for $\partial_z D$ yields

$$2\mu\partial_z D = \kappa\,\Omega'(z) - \overline{\Omega'(z)}\,, \tag{37}$$

where κ is given in (8). The complex displacement

$$2\mu D(z,\bar{z}) = \kappa\,\Omega(z) - z\,\overline{\Omega'(z)} - \overline{\omega(z)}\,, \tag{38}$$

is immediately obtained by inspection of (37) where the unknown function $\omega(z)$ has been introduced via its complex conjugate to conform with the conventions used in Ref. [9].

Note that (38) is the general solution to (35) and the unknown functions $\Omega(z)$ and $\omega(z)$ must be fixed by the boundary conditions. The displacement is chosen to vanish at the interface between the resin and the silica particle and this will allow us to eliminate $\omega(z)$ (we will return to this point shortly).

As noted in Section 4, it is convenient to endow the resin with a finite height h out of the plane and, from this perspective, a curve in the complex plane is equivalent to a ribbon of height h. The contact force per unit area f_j exerted at a point on the resin by the elastic loop is $f_j = \sigma_j{}^k n_k$, where the unit normal n_k points towards the loop. The boundary condition that we will use to determine $\Omega(z)$ is given by the requirement that the contact force per unit area exerted by the resin on the elastic loop must be equal and opposite to the contact force per unit area exerted by the loop on the resin. Expressing σ_{jk} in terms of the complex displacement leads to

$$\sigma_{11} + \sigma_{22} = 2(\lambda + \mu)(\partial_z D + \overline{\partial_z D}) + 2\beta, \tag{39}$$

$$\sigma_{11} - \sigma_{22} = 2\mu(\partial_z \overline{D} + \partial_{\overline{z}} D), \tag{40}$$

$$\sigma_{12} = i\mu(\partial_z \overline{D} - \partial_{\overline{z}} D)\,, \tag{41}$$

which, combined with (38), yield

$$\sigma_{11} + i\sigma_{12} = \Omega'(z) + \overline{\Omega'(z)} - z\,\overline{\Omega''(z)} - \overline{\omega'(z)} + \beta, \tag{42}$$

$$\sigma_{22} - i\sigma_{12} = \Omega'(z) + \overline{\Omega'(z)} + z\,\overline{\Omega''(z)} + \overline{\omega'(z)} + \beta. \tag{43}$$

The geometry of the outer component of the boundary of the resin is specified by the simple closed curve $z = Z(s)$ where s is the arc parameter of the curve, and we choose Z to be oriented in the anti-clockwise sense. The tangent to the curve is dZ/ds and it follows that the outward-pointing normal is $n = -idZ/ds$ where $n = n_1 + in_2$. Using (42), (43) with $f_j = \sigma_j{}^k n_k$ yields the remarkably compact expression

$$f = -i\frac{d}{ds}\left(\Omega(Z) + Z\,\overline{\Omega'(Z)} + \overline{\omega(Z)} + \beta Z\,,\right), \tag{44}$$

for the force per unit area exerted by the elastic loop on the resin, where $f = f_1 + if_2$.

A.1 Boundary condition at the resin-particle interface

For simplicity, the silica particle is assumed to be rigid in comparison with the resin and the elastic loop. Thus, the displacement (38) must vanish on the curve $(z-c)(\overline{z}-\overline{c}) = a^2$ where c is the centre of the particle and a is the radius of the particle. A simple way to enforce this condition is to analytically continue Ω into the disc occupied by the silica particle and choose

$$\omega(z) = \kappa\,\overline{\Omega\left(\frac{a^2}{\overline{z}-\overline{c}} + c\right)} - \left(\frac{a^2}{z-c} + \overline{c}\right)\Omega'(z). \tag{45}$$

Note that $\Omega(z)$ is chosen to be analytic everywhere within the outer component of the boundary of the resin, i.e. within the simple closed curve $z = Z(s)$.

A.2 Boundary condition at the resin-loop interface

The width of the cross-sections of the elastic loop are assumed to be much less than the other length scales in the system. Thus, for simplicity, we identify the outer component of the boundary of the resin with the space curve representing the loop and neglect shear forces within the loop. The loop then satisfies the balance law

$$\frac{d\boldsymbol{N}}{ds} + \boldsymbol{F} = 0\,, \tag{46}$$

associated with an elastic string (see, e.g. [11]) and the contact force $\boldsymbol{N}$ is given by

$$\boldsymbol{N} = \mathcal{T}\,\widehat{\frac{d\boldsymbol{R}}{ds}}\,, \tag{47}$$

where $\mathcal{T}$ is the tension in the loop, $\boldsymbol{R}(s)$ is the space curve describing the shape of the loop, s is the arc parameter of the loop in the undeformed state and

$$\widehat{\frac{d\boldsymbol{R}}{ds}} = \frac{1}{|d\boldsymbol{R}/ds|}\frac{d\boldsymbol{R}}{ds}. \tag{48}$$

The tension is specified in terms of the stretch $|d\boldsymbol{R}/ds|$ and we will adopt the simplest choice: the linear stress-strain relationship

$$\mathcal{T}(s) = EA(s)\left(\left|\frac{d\boldsymbol{R}}{ds}\right| - 1\right), \tag{49}$$

where the loop has Young's modulus E and $A(s)$ is the area of the cross-section of the loop labelled by s. The vector $\boldsymbol{F}$ in (46) is the force per unit reference length exerted on the loop by the resin; thus

$$\boldsymbol{F} = -h\,(f_1\hat{\boldsymbol{x}} + f_2\hat{\boldsymbol{y}})\,, \tag{50}$$

since $f = f_1 + if_2$ is the force per unit area exerted by the resin on the loop and h is the height of the cross-sections.

The outer component of the boundary of the resin in the undeformed state is the curve $z = Z(s)$ and so the point labelled by s is located at $Z(s) + \mathcal{D}(s)$ in the deformed state where

$$\mathcal{D}(s) = D\big(Z(s), \overline{Z(s)}\big). \tag{51}$$

Thus,

$$\boldsymbol{R}(s) = \mathrm{Re}[Z(s) + \mathcal{D}(s)]\hat{\boldsymbol{x}} + \mathrm{Im}[Z(s) + \mathcal{D}(s)]\hat{\boldsymbol{y}}, \tag{52}$$

and

$$\mathcal{T}(s) = EA(s)\,\mathrm{Re}\left(\frac{d\overline{Z}}{ds}\frac{d\mathcal{D}}{ds}\right), \tag{53}$$

follows from (49), (52) to first order in the displacement $\mathcal{D}$ and its derivatives; hence

$$\begin{aligned}\hat{\boldsymbol{x}}\cdot\boldsymbol{N} + i\hat{\boldsymbol{y}}\cdot\boldsymbol{N} &= \mathcal{T}\left(\hat{\boldsymbol{x}}\cdot\widehat{\frac{d\boldsymbol{R}}{ds}} + i\hat{\boldsymbol{y}}\cdot\widehat{\frac{d\boldsymbol{R}}{ds}}\right)\\ &= \mathcal{T}\,\frac{dZ}{ds}\end{aligned} \tag{54}$$

to first order in the displacement $\mathcal{D}$ and its derivatives. Thus, (44), (46), (50) and (54) yield

$$\frac{d}{ds}\left(\mathcal{T}\,\frac{dZ}{ds}\right) + ih\frac{d}{ds}\left(\Omega(Z) + Z\,\overline{\Omega'(Z)} + \overline{\omega(Z)} + \beta Z\right) = 0\,, \tag{55}$$

to first order in the displacement $\mathcal{D}$ and its derivatives. Equation (5) is obtained by integrating (55), setting the constant of integration to zero and eliminating $\omega(Z)$ using (38) and (51).

A.3 Fixing the constant β

The thermo-elastic behaviour of a disc of unconstrained resin can be easily explored by setting $\omega(z) = 0$ and solving the free surface boundary condition

$$\Omega(Z) + Z\,\overline{\Omega'(Z)} + \beta Z = 0 \tag{56}$$

for Ω, where $Z(s) = b\exp(is/b)$ and b is the radius of the disc (see (44) with $\omega(z) = 0$). On grounds of symmetry, $\Omega(z) = \alpha_1 z$ and $D(z, \overline{z}) = \delta_1 z$ where $\mathrm{Im}(\delta_1) = 0$; hence (38) yields

$$2\mu\delta_1 = \kappa\alpha_1 - \overline{\alpha_1} \tag{57}$$

and $\mathrm{Im}(\alpha_1) = 0$ is an immediate consequence. Thus

$$\delta_1 = \frac{-(\kappa - 1)\beta}{4\mu} \tag{58}$$

where α_1 has been eliminated using (56), and the change

$$\pi(b + \delta_1)^2 - \pi b^2 = \frac{-(\kappa - 1)\beta}{2\mu}\pi b^2 + \mathcal{O}(\delta_1^2) \tag{59}$$

in area of the disc follows to first order in δ_1. Hence, the identification

$$\beta = \frac{-2\mu}{(\kappa - 1)}\alpha(T - T_0) \tag{60}$$

emerges from (59) where α is the coefficient of thermal expansion of the resin, T is the temperature of the resin and T_0 is the temperature of the resin in the undeformed state. Equation (10) is obtained using (8), (9), and (60).

6 References

[1] S. Timoshenko. Analysis of bi-metal thermostats. *J. Opt. Soc. Am.*, 11(3):233–255, 1925.

[2] E. Suhir. Stresses in bimetal thermostats. *J. Appl. Mech.*, 53(3):657–660, 1986.

[3] E. Suhir. Interfacial stresses in bimetal thermostats. *J. Appl. Mech.*, 56(3):595–600, 1989.

[4] D. Sujan, Z. Oo, M. V. V. Murthy, and K. N. Seetharamu. Effect of different uniform temperature with thickness-wise linear temperature gradient on interfacial stresses of a bi-material assembly. *Am. J. Applied Sci.*, 7(6):829–834, 2010.

[5] D. J. Acheson. *Elementary Fluid Dynamics.* Oxford University Press, 2nd edition, 1990.

[6] P. G. Saffman. *Vortex Dynamics.* Cambridge University Press, 2nd edition, 1995.

[7] D. A. Burton, J. Gratus, and R.W. Tucker. Hydrodynamic forces on two moving discs. *Theor. Appl. Mech.*, 31(2):153–188, 2004.

[8] D.G. Crowdy. Analytical solutions for uniform potential flow past multiple cylinders. *Eur. J. Mech. B-Fluid*, 25(4):459–470, 2006.

[9] A. H. England. *Complex Variable Methods in Elasticity.* Dover Publications, 1st edition, 2003.

[10] L.D. Landau and E.M. Lifshitz. *Theory of Elasticity (Course of Theoretical Physics, Volume 7).* Pergamon, 2nd edition, 1970.

[11] S. S. Antman. *Nonlinear Problems of Elasticity (Applied Mathematical Sciences 107).* Springer, 2nd edition, 2004.